An Application of the Moment Method to Waveguide Scattering Problems

SIEN-CHONG WU AND Y. LEONARD CHOW

Abstract—**A moment method is suggested to solve scattering problems in waveguides. It takes advantage of the localized nature of the evanescent waves to assure the convergence of the solutions. The method chooses the point-matching approach with pulse basis functions so that it may be versatile and can be applied to discontinuities of an arbitrary shape. To illustrate this method, examples are given for open-ended parallel-plane waveguides, both flanged and unflanged, and for waveguides with obstacles of various shapes. Comparisons are made with solutions by other approaches and, whenever possible, with exact solutions. The agreements are good.**

I. Introduction

PROBLEMS of scattering by discontinuities in waveguides have been widely studied in the past decade. Except for a few special discontinuities, exact solutions are not available and approximate methods have to be used. The ray theory has been applied to the regularly shaped discontinuities in a waveguide by Yee and Felsen [1]. A similar theory has also been applied to open-ended waveguides, both flanged and unflanged, by Lee [2], Yee, Felsen, and Keller [3] as well as Rudduck and Tsai [4]. For flanged waveguides, Itoh and Mittra have been able to give a more rigorous solution by a modified residue calculus technique [5].

All the above approximate methods are restricted to regular discontinuities such as sharp edges linked by reasonably long and straight boundaries. A more versatile method is needed for arbitrary boundaries and closely spaced edges. In open space, the moment method has been applied to solve scattering problems of obstacles with finite sizes [6]. The extension to scattering by a semi-infinite plate has recently been made by Morita [7]. Using a similar procedure, this investigation further extends the moment method to the closed space inside a waveguide which has infinitely long walls along the propagation direction.

The procedure is the following: first, the propagating wave in a waveguide is considered to be a plane wave bouncing off the walls of the waveguide. When this bouncing wave meets the discontinuity, the scattered field occurs. This field is then decomposed into the reflected, transmitted, and evanescent waves. The reflected and transmitted waves are again represented by plane waves with the reflection and transmission coefficients R and T. The evanescent wave is represented by the extra induced current density on the conducting surfaces which is localized at the discontinuity. The moment method with the point-matching approach [6] can then be applied to solve the coefficients R and T and the induced current density. The basis functions of the method are kept simple in the form of unit pulses. The approach and the basis functions are chosen to prepare the moment method for an arbitrarily shaped discontinuity. The convergence from such procedure is assured since the effects of the induced currents from the plane waves are analytically integrable and the basis functions are needed only to numerically calculate the effects of the evanescent wave. As the evanescent wave decays exponentially from the discontinuity, the basis functions are required to cover only a finite space. This has the effect of reducing the infinitely long walls of the waveguide to finite ones.

Manuscript received November 19, 1971; revised June 30, 1972. This work was supported by the National Research Council of Canada under Grant A3804.

The authors are with the Department of Electrical Engineering, University of Waterloo, Waterloo, Ont., Canada.

II. Formulation

Let us assume that a TE_{01} mode wave propagates in a parallel-plane waveguide of infinite extent. The field can be considered to be a plane wave bouncing off the upper and the lower waveguide walls with an angle $\theta = \sin^{-1}(\lambda/2d)$ as shown in Fig. 1. The fields of the plane-wave incident on the lower waveguide wall can be written as

$$\boldsymbol{E}^i = \hat{z} \exp\left[jk(x\cos\theta + y\sin\theta)\right] \tag{1}$$

and

$$\boldsymbol{H}^i = (-\hat{x}\sin\theta + \hat{y}\cos\theta)\frac{1}{\eta}\exp\left[jk(x\cos\theta + y\sin\theta)\right] \tag{2}$$

where $\eta = (\mu/\epsilon)^{1/2}$ is the intrinsic impedance of the medium in the waveguide. On the lower waveguide wall a current density

$$J^i = \hat{z}\frac{2}{\eta}\sin\theta\exp(jkx\cos\theta) \tag{3}$$

is induced. The current density induced on the upper wall is identical to that on the lower wall.

If an obstacle is located in the waveguide, a fraction of the incident field is reflected and the remainder trans-

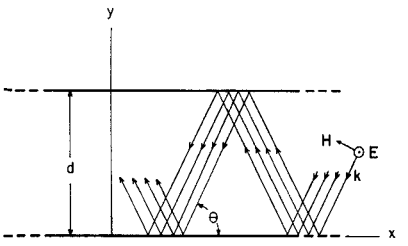

Fig. 1. Propagating plane wave in a parallel-plane waveguide.

mitted. For simplicity, we shall limit the spacing between the two plates d such that all higher modes are cut off. The current densities induced by the reflected and transmitted waves, with coefficients R and T, are

$$J^r = \hat{z}R\frac{2}{\eta}\sin\theta\exp(-jkx\cos\theta), \qquad x>0,\ y=0, \quad \text{and} \quad y=d \tag{4}$$

and

$$J^t = \hat{z}T\frac{2}{\eta}\sin\theta\exp(jkx\cos\theta), \qquad x<0,\ y=0, \quad \text{and} \quad y=d. \tag{5}$$

In addition, a current density $J^e=\hat{z}J_z^e$ corresponding to the evanescent wave exists at, and in the vicinity of, the discontinuity. Each of these current-density components contributes to the transverse E-field in the waveguide. In order to satisfy the boundary condition that tangential electric field E_z vanishes on a conductor, the following integral equation is established [6]:

$$0=\frac{\eta}{4}\int_c J_z^e(r')H_0^{(2)}(k\,|\,r-r'\,|)d(kr')+\frac{\eta}{4}\int_w [J_z^i(r')+J_z^r(r')+J_z^t(r')]H_0^{(2)}(k\,|\,r-r'\,|)d(kr') \tag{6}$$

where r and r' are the coordinates of the field points and of the source points on the conductor. The integral path c is along the surface of the obstacle and the nearby waveguide walls and the integral path w is along all relevant waveguide walls, i.e., to the right of the discontinuity for J_z^i and J_z^r, and to the left for J_z^t.

With arbitrary obstacles, (6) cannot be solved exactly. The moment method can, however, be used to obtain an approximate solution. First, we shall choose the point-matching approach with basis functions in the form of unit pulses. This is in effect dividing the integral path c into N segments each with an unknown current density J_n [6]. Substituting (3), (4), and (5) into (6) we have a linear equation with $N+2$ unknowns, J_1, J_2, $\cdots$, J_N, R, and T. The required $N+2$ test field points are selected on the conductor so that N of them coincide with the N source points at the centers of the segments along c, and another two at distant points along the walls. Therefore $N+2$ linear equations are established and can be written in the following matrix form [6]:

$$[l_{m,n}][f_m]=[g_m] \tag{7}$$

where $l_{m,n}$, f_m, and g_m will be given below.

For the operator elements $l_{m,n}$, with $m=1, 2, \cdots, N+2$ and with $n=1, 2, \cdots, N$, we have

$$l_{m,n}=H_0^{(2)}(k\,|\,r_m-r'_n\,|)\Delta(kr_n'), \qquad \text{if } m\neq n \tag{8}$$

$$l_{m,n}=\left[1-j\frac{2}{\pi}\left(\ln\frac{\Delta(kr_n')}{4}+\gamma-1\right)\right]\Delta(kr_n'), \qquad \text{if } m=n \tag{9}$$

with $\gamma=0.5772157\cdots$. In addition, with $n=N+1$ and $N+2$ corresponding to R and T, we have

$$l_{m,N+1}=\frac{\sin\theta}{2}[I_-(0,\infty,y_m)+I_-(0,\infty,d-y_m)] \tag{10}$$

$$l_{m,N+2}=\frac{\sin\theta}{2}[I_+(-\infty,0,y_m)+I_+(-\infty,0,d-y_m)] \tag{11}$$

where

$$I_\pm(a,b,y)=\int_a^b \exp(\pm jkx'\cos\theta)H_0^{(2)}\cdot[k((x'-x_m)^2+y^2)^{1/2}]d(kx'). \tag{12}$$

For incident field elements g_m and other induced field elements f_m we have

$$g_m=-\frac{\sin\theta}{2}[I_+(0,\infty,y_m)+I_+(0,\infty,d-y_m)] \tag{13}$$

and

$$f_m=\begin{cases}\frac{\eta}{4}J_m, & \text{for } m=1,2,\cdots,N\\ R, & \text{for } m=N+1\\ T, & \text{for } m=N+2.\end{cases} \tag{14}$$

The analytical integrals $I_\pm$ in (10), (11), and (12) are of a semi-infinite type with very slow convergence. Before numerical computations they should be converted into a more convenient form. First, the replacement of x' by $-x'$ in (12) changes the integration limits in (11) into $(0,\infty)$. Then all the six integrals above have a similar form of $I_\pm(0,\infty,y)$. With $X=kx'$, $X_m=kx_m$, and $Y=ky_m$ or $k(d-y_m)$, the integrals can in turn be divided into two parts, that is

$$I_\pm=\exp(\pm jX_m\cos\theta)\left\{\int_{-X_m}^0 \exp(\pm jX\cos\theta)H_0^{(2)}\cdot[(X^2+Y^2)^{1/2}]dX+\int_0^\infty \exp(\pm jX\cos\theta)H_0^{(2)}\cdot[(X^2+Y^2)^{1/2}]dX\right\}. \tag{15}$$

It has been shown by Morita [7] that with the lower sign the second integral of the above can be written as

$$\int_0^\infty \exp(-jX\cos\theta)H_0^{(2)}[(X^2+Y^2)^{1/2}]dX$$
$$= -j\int_0^Y \exp(-X\cos\theta)H_0^{(2)}[(Y^2-X^2)^{1/2}]dX$$
$$+\frac{2}{\pi}\exp(-Y\cos\theta)$$
$$\cdot\left\{\frac{1}{2\cos\theta}\left(-\gamma+\ln\frac{2\cos\theta}{Y}-\frac{1}{2Y\cos\theta}\right)\right.$$
$$+\int_0^\infty\left[K_0((X^2+2YX)^{1/2})+\gamma\right.$$
$$\left.\left.+\frac{1}{2}\ln\frac{YX}{2}+\frac{X}{4Y}\right]\exp(-X\cos\theta)dX\right\}. \quad (16)$$

The last integral in (16) is a standard form of Gauss–Laguerre quadrature which is easily computable [8].

Also with the upper sign the second integral in (15) can be reduced to

$$\int_0^\infty \exp(jX\cos\theta)H_0^{(2)}[(X^2+Y^2)^{1/2}]dX$$
$$=\int_{-\infty}^\infty \exp(jX\cos\theta)H_0^{(2)}[(X^2+Y^2)^{1/2}]dX$$
$$-\int_{-\infty}^0 \exp(jX\cos\theta)H_0^{(2)}[(X^2+Y^2)^{1/2}]dX$$
$$=\frac{2}{\sin\theta}\exp(-jY\sin\theta)$$
$$-\int_0^\infty \exp(-jX\cos\theta)H_0^{(2)}[(X^2+Y^2)^{1/2}]dX. \quad (17)$$

The second term of the reduced form is actually the integral of the left-hand side of (16). Therefore, with the help of (16) and (17), the integrals in (10), (11), and (13) are all convertible to integrals which can be numerically computed.

In many applications $Y=0$, and (16) and (17) are analytically integrable. They are, respectively,

$$\int_0^\infty \exp(-jX\cos\theta)H_0^{(2)}(X)dX=\frac{2\theta}{\pi\sin\theta} \quad (18)$$

and

$$\int_0^\infty \exp(jX\cos\theta)H_0^{(2)}(X)dX=\frac{2(\pi-\theta)}{\pi\sin\theta}. \quad (19)$$

With either analytical or numerical integrations of (10), (11), and (13), all of the $l_{m,n}$ and g_m are determined and may be substituted into (7). Then by matrix inversion we may solve for the reflection and transmission coefficients R and T.

III. Numerical Examples

A. Transverse Diaphragm

As the first example, let us consider a perfectly conducting, thin, transverse diaphragm located on the lower wall of a parallel-plane waveguide as shown in Fig. 2. The height of this diaphragm is h. The coordinates are chosen that the origin coincides with the base of the diaphragm. A TE_{01} mode wave is incident from $x=\infty$ toward the diaphragm. Since the diaphragm is thin and is symmetrical with respect to the $x=0$ plane, the diffracted current density in the vicinity of the diaphragm is also symmetrical. Therefore, we need to calculate only the diffracted current density on the diaphragm and on the waveguide walls for $x>0$.

The scattered wave propagating in the $x>0$ region corresponds to the reflected wave, while that propagating in the $x<0$ region, together with the incident wave, corresponds to the transmitted waves. In the case of propagating TE_{01} mode only (i.e., $\lambda/2<d<\lambda$) we can put

$$T=1+R. \quad (20)$$

Hence T, the $(N+2)$th unknown in (14), may be eliminated. Under this circumstance, the incident wave may be conveniently considered to propagate along the whole waveguide, instead of only in the $x>0$ region, and the reflected wave to propagate from the diaphragm at $x=0$ toward both the $x>0$ and the $x<0$ regions. Hence $l_{m,N+1}$ in (10) may be replaced by the sum of $l_{m,N+1}$ and $l_{m,N+2}$ in (10) and (11), and the integration limits in (13) may be extended to $(-\infty,\infty)$. In such cases g_m in (13) becomes the transverse E-field at a point (x_m, y_m) in an infinitely long waveguide, and thus has the simple form

$$g_m=j2\sin(ky_m\sin\theta)\exp(jkx_m\cos\theta). \quad (21)$$

With all of the matrix elements derived, the solution of the reflection coefficient R is computed by (7) and is plotted in Fig. 2 for $h=d/2$ and $\lambda/2\leq d\leq\lambda$. Exact solution, as calculated from the procedure given in Collin [9], is included for comparison. Also given in the figure is solution obtained by Yee and Felsen (i.e., YF solution) [1]. Excellent agreement is observed between the results from the present approach and the exact solution. The agreement is better, in the particular range $\lambda/2\leq d\leq\lambda$, than that of the YF solution, especially in the regions near the cutoff frequencies where the YF solution does not apply.

B. Open-Ended Parallel-Plane Waveguide

Next, we consider an infinitely thin parallel-plane waveguide with one end open to the free space, as

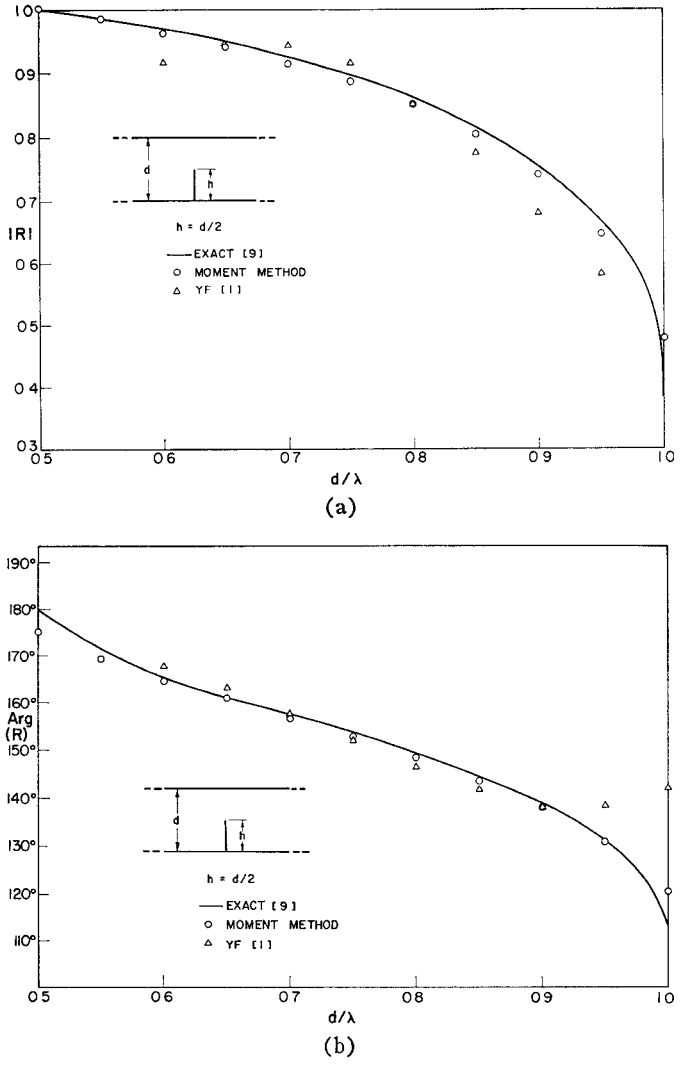

Fig. 2. The reflection coefficient of a parallel-plane waveguide with a transversal diaphragm. (a) Magnitude. (b) Phase.

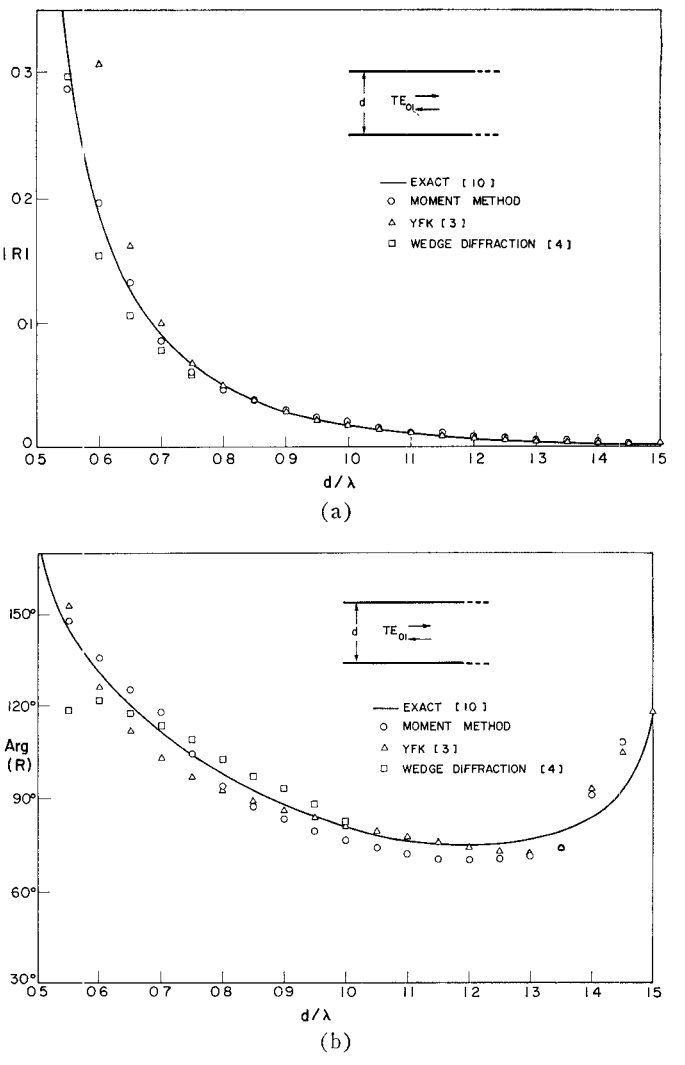

Fig. 3. The reflection coefficient of an infinitely thin open-ended parallel-plane waveguide. (a) Magnitude. (b) Phase.

shown in Fig. 3. A TE_{01} mode wave is propagating in the waveguide toward the open end. In this case the "discontinuity" is symmetrical with respect to the axial plane so that with $\lambda/2 < d < 3\lambda/2$ the waveguide will retain only the TE_{01} mode in the reflected wave. Furthermore, the diffracted current density on the upper wall is identical to that on the lower wall. This allows us to calculate only the current density on the lower wall, and the reflection coefficient R. In doing so, $l_{m,n}$ in (8) and (9) are modified to the following forms:

$$l_{m,n} = \{H_0^{(2)}(k|x_m - x_n'|) + H_0^{(2)} \cdot [k((x_m - x_n')^2 + d^2)^{1/2}]\}\Delta(kx_n'), \qquad m \neq n \quad (22)$$

$$l_{m,n} = \left\{1 - j\frac{2}{\pi}\left[\ln\frac{\Delta(kx_n')}{4} + \gamma - 1\right] + H_0^{(2)}(kd)\right\}\Delta(kx_n'), \qquad m = n. \quad (23)$$

Also, the $x < 0$ region is occupied by free space and J^t in (5) vanishes. Hence the transmission coefficient T does not appear. This requires the dropping of (11) and leaving only $N+1$ unknowns to be solved. In addition since the discontinuity is everywhere along the waveguide walls, the point coordinates y_m and y_n are all zero; hence they have been dropped from the $l_{m,n}$ and g_m in (10), (13), (22), and (23).

In the case of the flanged open-ended waveguide in Fig. 4, additional segments (i.e., test points) are needed to take the diffracted current densities on the flanges into account. However, it is found that these diffracted current densities decay very rapidly along the flanges and, therefore, only a few additional points are necessary. Note that at these additional points the y_m and y_n are not zero and will appear in the additional $l_{m,n}$ and g_m.

The computed reflection coefficients for both flanged and unflanged waveguides are plotted in Figs. 3 and 4.

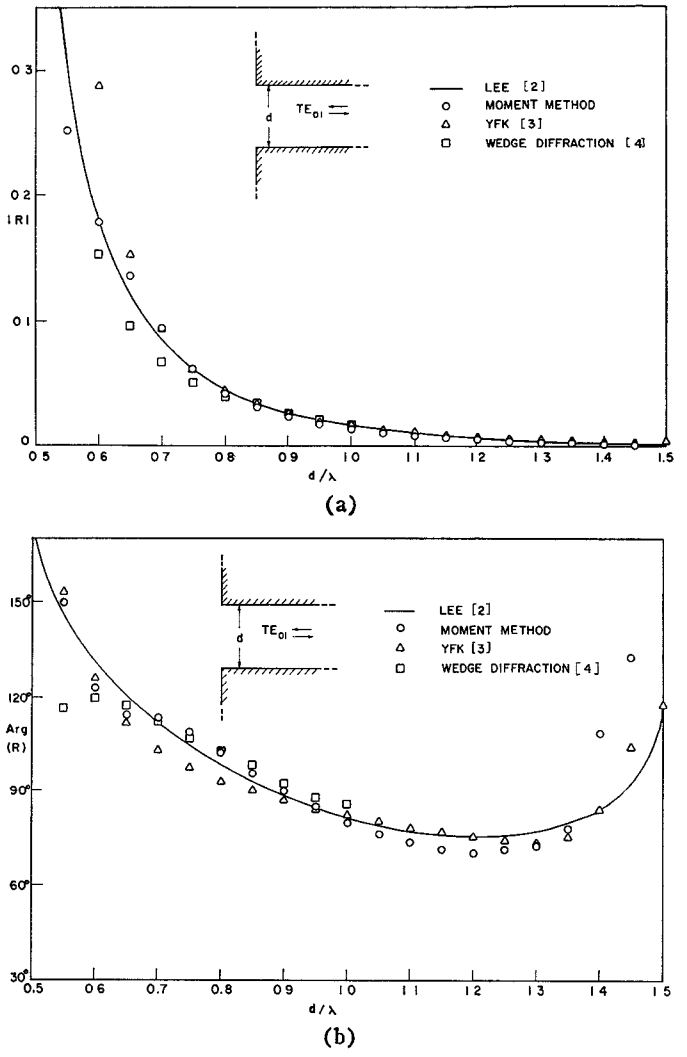

Fig. 4. The reflection coefficient of an open-ended parallel-plane waveguide with flanges. (a) Magnitude. (b) Phase.

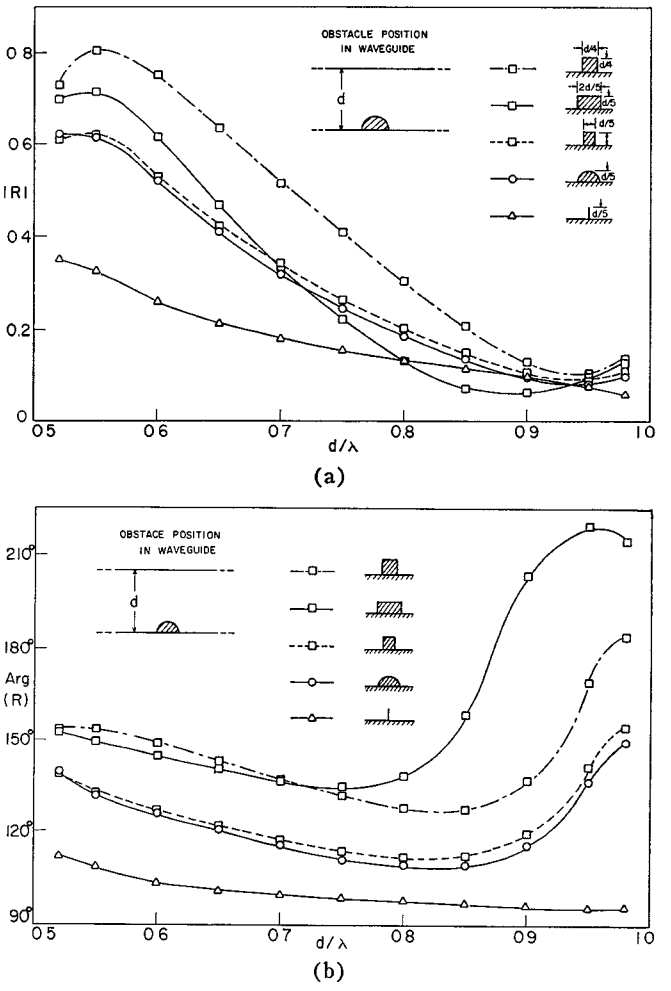

Fig. 5. The reflection coefficients of a parallel-plane waveguide with obstacles of different shapes. (a) Magnitudes. (b) Phases. The phases of the coefficients are measured from the centers of the obstacles.

The exact solution for the unflanged waveguide by the Wiener–Hopf technique [10] is included for comparison. The exact solution for the flanged waveguide is not available. In its place, Lee's solution [2] is substituted since the latter solution appears to be more rigorous than other approximate solutions for TE modes.

Solutions by other approximation techniques, such as those by the YFK method [3] and by wedge diffraction theory [4], are also given in the figures. From these figures it appears that present approach gives very good results, especially in the normal operating range of $\lambda/2 < d < \lambda$. As the spacing d exceeds a wavelength the reflection coefficients become small and, as a result, the phase errors in computation become large [cf. Figs. 3(b) and 4(b)].

C. Thick Obstacles

Thus far we have considered discontinuities with sharp edges. In order to show the versatility of the moment method, thick obstacles of various shapes in a waveguide are considered. It is noted that for thick obstacles, and other obstacles in general, the diffraction fields are *not* symmetrical on both sides of the obstacle. Hence in spite of the similarity between some of the examples in Fig. 5 and the thin transverse diaphragm, the simplification introduced for the thin transverse diaphragm cannot be used here. Instead, the complete formulation given in (7)–(14) is used.

The solutions for five different obstacles are shown in Fig. 5. No comparisons are given for lack of available solutions by other methods. However, in view of the accuracy of the solutions given in the preceding two examples, it is expected that these solutions are reasonably accurate.

IV. Discussion

The above examples have shown that the moment method, of the point-matching approach and with pulse basis functions, can be applied to solve scattering problems in waveguides. The procedure is kept simple so that the moment method can be applied to discontinuities of any shape. The convergence of this procedure is assured since the evanescent waves from the discontinuities are normally highly localized (say, $kr < 10$).

In the above examples, each segment (i.e., basis function) for operator elements $l_{m,n}$ in (8) and (9) has been subdivided into three subsegments, with weighting approximating a triangle function as suggested by Harrington [6]. In doing so, the $l_{m,n}$ are more accurate and the number of segments can be reduced by one half without an apparent increase in error. In fact, in all the examples above, no more than 30 segments are used on both the discontinuity and the waveguide walls.

For simplicity and for comparison with the available exact solutions, only the fundamental TE_{01} mode has been assumed propagating. It is easy to see, however, that higher TE_{0N} modes can also be assumed to propagate without unduly increasing the computation time. For each additional mode, two field elements f_m, corresponding to the reflection and transmission coefficients of the additional mode, are needed. The extra computation is therefore not much more than required by having two extra segments on the waveguide walls.

Finally, it is to be pointed out that the present method, as well as most other numerical methods, is suitable for treating waveguide with electrically small dimensions. As the guide gets larger, the ray optics method [1]–[4] becomes superior.

References

[1] H. Y. Yee and L. B. Felsen, "Ray optics—A novel approach to scattering by discontinuities in a waveguide," *IEEE Trans. Microwave Theory Tech.*, vol. MTT-17, pp. 73–85, Feb. 1969.

[2] S. W. Lee, "Ray theory of diffraction by open-ended waveguides. Part I," *J. Math. Phys.*, vol. 11, pp. 2830–2850, Sept. 1970.

[3] H. Y. Yee, L. B. Felsen, and J. B. Keller, "Ray theory of reflection from the open end of a waveguide," *SIAM J. Appl. Math.*, vol. 16, pp. 268–301, Mar. 1968.

[4] R. C. Rudduck and L. L. Tsai, "Aperture reflection coefficient of TEM and TE_{01} mode parallel-plate waveguides," *IEEE Trans. Antennas Propagat.*, vol. AP-16, pp. 83–89, Jan. 1968.

[5] T. Itoh and R. Mittra, "A new method of solution for radiation from a flanged waveguide," *Proc. IEEE* (Lett.), vol. 59, pp. 1131–1133, July 1971.

[6] R. F. Harrington, *Field Computation by Moment Methods*. New York: Macmillan, 1968, pp. 41–49.

[7] N. Morita, "Diffraction by arbitrary cross-sectional semi-infinite conductor," *IEEE Trans. Antennas and Propagat.*, vol. AP-19, pp. 358–364, May 1971.

[8] Z. Kopal, *Numerical Analysis*. New York: Wiley, 1961, ch. 7.

[9] R. E. Collin, *Field Theory of Guided Waves*. New York: McGraw-Hill, 1960, pp. 441–450.

[10] L. A. Vaynshteyn, *The Theory of Diffraction and the Factorization Method*. Boulder, Colo.: Golem, 1969, ch. 1.

Diffraction of a Wave Beam by an Aperture

KAZUMASA TANAKA, MASARU SHIBUKAWA, AND OTOZO FUKUMITSU

Abstract—**The diffraction field of a wave beam from a circular and a rectangular aperture is obtained in the Fresnel region by using the Huygens–Kirchhoff approximation. The diffraction field in the Fraunhofer region can be obtained simply by replacing a parameter. The diffraction field is then expanded into a series of beam mode functions.**

From the field distributions and the expansion coefficients, which represent the coupling of the incident beam to the various modes in the diffraction field, the effects of an aperture on the incident beam can be known. With this mode expansion method, the conditions for optimum coupling between fundamental modes are obtained and solved numerically.

I. Introduction

THE output wave beam from optical structures, like Fabry–Perot resonators or optical transmission lines, can be described by Hermite–Gaussian [1] or Laguerre–Gaussian [2] functions.

Apertures, such as irises, are often used as elements of these structures, but there have been few papers that discussed the effects of an aperture on the wave beam. Only the diffraction losses due to the finite sizes of the lens, or mirror apertures that are used as elements of transmission lines [2] or of resonators [3], have been discussed.

The diffraction from an aperture is one of the fundamental problems in electromagnetic field theory and many detailed theories have been compiled for plane wave or spherical wave incidence. The main reason why the diffraction problem for a wave beam has not yet been discussed may be explained by the complexity of the beam wave functions. Up to the present knowledge of the diffraction field of plane waves has been applied to this case.

But, as is well known, if a wave beam of an optical structure is incident on another system, a set of modes of the system is excited or the parameters of the incident wave beam are transformed into different beam parameters [4]. For example, a thin lens transforms these parameters from one set to another. These effects cannot be explained by the analogy of plane wave diffraction.

For this reason, the diffraction problems of a wave beam from a circular and a rectangular aperture are dis-

Manuscript received March 8, 1972; revised June 1, 1972.

K. Tanaka is with the Department of Electrical Engineering, Nagasaki University, Nagasaki, Japan.

M. Shibukawa and O. Fukumitsu are with the Department of Computer Science and Communication Engineering, Kyushu University, Fukuoka, Japan.